

# Development of a Graphene Based Electrochemical Sensor for the Determination of 9-hydroxyrisperidone in Human Blood Plasma

Wenying Zhang\* and Yanping Wang

Department of Laboratory Medicine, Tianjin Anding Hospital, Tianjin, 300222, P.R. China

\*E-mail: [wenyingzhangsally@163.com](mailto:wenyingzhangsally@163.com)

*Received:* 15 November 2017 / *Accepted:* 4 January 2018 / *Published:* 5 February 2018

---

This work reports the preparation of a 9-hydroxyrisperidone amperometric biosensor using a glassy carbon electrode (GCE) modified with reduced graphene oxide wrapped hierarchical TiO<sub>2</sub> (RGO-TiO<sub>2</sub>) nanohybrid. In addition, the electro catalytic behaviour of the biosensor to the oxidation of 9-hydroxyrisperidone was studied using amperometric and cyclic voltammetry (CV) measurements. The low oxidation potential and enhanced current response of the RGO-TiO<sub>2</sub> modified GCE resulted from the synergistic effects of TiO<sub>2</sub> and RGO. For the analysis of the 9-hydroxyrisperidone, the developed biosensor has a low limit of detection (LOD) of 0.52 ng/mL and a wide linear detection range of 1 to 1500 ng/mL. Therefore, our developed biosensor had the potential for use in the practical detection of 9-hydroxyrisperidone in human blood plasma specimens.

---

**Keywords:** 9-hydroxyrisperidone; TiO<sub>2</sub>; Graphene; Human blood plasma; Electrochemical sensor

## 1. INTRODUCTION

As an atypical antipsychotic, risperidone acts via selective antagonism of serotonin 5-HT<sub>2</sub> and dopamine D<sub>2</sub> receptors [1-3]. Risperidone has a lower potential to cause extrapyramidal side effects compared to classical antipsychotics; it is effective in treating positive and negative symptoms of schizophrenia [4, 5]. Furthermore, it also has a role in the treatment of bipolar and schizoaffective disorders, as shown in recently reported open trial studies [6, 7]. Extensive 9-hydroxylation is often found for risperidone in the liver via cytochrome P450 isoenzymes (CYP), whereas 7-hydroxylation and *N*-dealkylation become less significant [8, 9]. CYP2D6 is the main catalyst for the generation of 9-hydroxyrisperidone [10-12], while the engagement of CYP3A4 has been reported in recent *in vitro* studies [13]. Considering the similar pharmacological activity of 9-hydroxyrisperidone and the parent compound, the “active moiety” usually refers to the sum of their plasma concentrations [14]. The

influencing factors on the plasma levels of the active moiety are impaired renal and hepatic function, CYP2D6 genotype, age, and a concomitant administration of other drugs [15, 16]. Although the plasma concentrations have not been reported to obviously correlate with the clinical effects [17, 18], it is still essential to monitor the plasma 9-hydroxyrisperidone and risperidone levels in certain cases.

Few studies have been reported for the analysis of 9-hydroxyrisperidone and risperidone in human serum or plasma and those include: specific radioimmunoassay (RIA) [19], high-performance liquid chromatography (HPLC) analysis with either ultraviolet [20, 21] or electrochemical [20, 22] determination after liquid–liquid extraction [23–25] and solid-phase extraction [26, 27]. A few of the HPLC routes are characterised by low LOD or low limit of quantitation (LOQ), although they require a long operation time. Specifically, the specimen cleaning involves a multi-step liquid–liquid extraction process that requires long procedures and/or reduced recovery [28, 29]. Additionally, some measurements suffer from prolonged chromatographic runs [11, 30].

With the development of nanotechnology and nanoscience, increasing attention has been paid to the preparation of point-of-care diagnostic tools for food safety, global health, and environmental monitoring [31, 32]. For the analysis of aptamers, PNA, smRNA, pathogens, etc., many excellent multifunctional nanomaterials have been reported [33, 34]. Functional groups such as carboxyl, carbonyl, epoxide, and hydroxyl are present on the planes/edges of a GO sheet and have been used to accelerate the conjugation of biomolecules or proteins during the preparation of biosensors [35–37].

Reduced graphene oxide (RGO) can be obtained by tuning the electrical conductivity of graphene oxide (GO) through chemical reduction. The RGO has a high density of edge-plane-like defects in addition to a large surface area, which allows for a more rapid heterogeneous charge transfer. Therefore, the electron carrier mobility and electrochemical features of RGO are higher than that for GO [38–40]. Additionally, RGO is also a mechanically flexible, synthetically inexpensive and easily processed material. As such, it has been utilised extensively in many different fields, such as photodetectors, photovoltaics, field effect transistors, biosensors, etc. Anatase TiO<sub>2</sub> (ant-TiO<sub>2</sub>), is non-toxic, has high biocompatibility, is inexpensive, has distinct oxidation properties, has long-term stability and has gained wide application [19]. In addition, TiO<sub>2</sub> nanoparticles are also capable of adsorbing desired proteins, as well as efficiently coordinating charge transfer between an electrode and protein molecules. The preparation of ant-TiO<sub>2</sub> and an RGO nanohybrid has been reported for the production of a potential electrochemical immunosensor [41, 42]. These two materials can be integrated via a direct self-assembly route, where the van der Waals interactions between the oxygen moiety (on the ant-TiO<sub>2</sub> surface) and the graphene basal plane would be enhanced. The electrochemical performance would also be promoted after homogeneously distributing the ant-TiO<sub>2</sub> nanoparticles onto the multi-layered RGO.

In the present report, a TiO<sub>2</sub> incorporated RGO nanohybrid (RGO-TiO<sub>2</sub>) was successfully prepared using a simple wet chemical technique. The electro catalytic activity of our developed RGO-TiO<sub>2</sub> modified glass carbon electrode (GCE) to the analysis of 9-hydroxyrisperidone was remarkable, with a low limit of detection (LOD) and a wide linear range. Additionally, the proposed biosensor was applied to the detection of human blood plasma specimens.

## 2. EXPERIMENTS

### 2.1. Chemicals

Graphene oxide powder was purchased from JCNANO, INC. Acetylcholine (Ach), glucose, 3-hydroxytyramine hydrochloride (DA), uric acid (UA), poly(diallyl dimethyl ammonium chloride) (PDDA, 20 wt.%), titanium butoxide, ascorbic acid, and 9-hydroxyrisperidone were purchased from Sigma-Aldrich. All reagents were analytical grade and used without further purification. For the preparation of the phosphate buffer solution (PBS), a 0.1 M solution of  $K_2HPO_4$  and  $KH_2PO_4$  was mixed together to a target pH value. Deionised water, 18.2 M $\Omega$  cm milli-Q, was used for all the following measurements.

### 2.2. Preparation of RGO-TiO<sub>2</sub> nanocomposite

A simple hydrothermal strategy (Lui et al. 2013) was modified and used for the preparation of TiO<sub>2</sub> nanoballs in our case. In brief, acetic acid (20 mL) was mixed with titanium butoxide (2 mL) and stirred for 30 min. The obtained mixture was transferred to a 50 mL Teflon-lined stainless steel autoclave, followed by heating up to 150 °C in an oven for 10 h. After cooling to ambient temperature, the sediment was centrifuged and collected. After washing and heating at 500 °C, the TiO<sub>2</sub> nanoballs were produced. For the synthesis of the RGO-TiO<sub>2</sub> nanohybrid, 100 mg of the prepared TiO<sub>2</sub> nanoballs were dispersed into 20 mL water and sonicated; this was followed by the addition of PDDA (2 mL), and that mixture was stirred for 2 h. After centrifugation and a water wash, the PDDA functionalised TiO<sub>2</sub> was obtained and followed by re-dispersion into 20 mL of water. This PDDA functionalised TiO<sub>2</sub> was then mixed with 2 mL of a 1 mg/mL GO dispersion and stirred for 60 min. This dispersion was further mixed with an ammonia solution (2 mL), transferred to a 50 mL Teflon-lined stainless steel autoclave and heated at 120 °C for 2 h. After centrifugation, the RGO-TiO<sub>2</sub> nanohybrid was collected.

### 2.3. Characterization

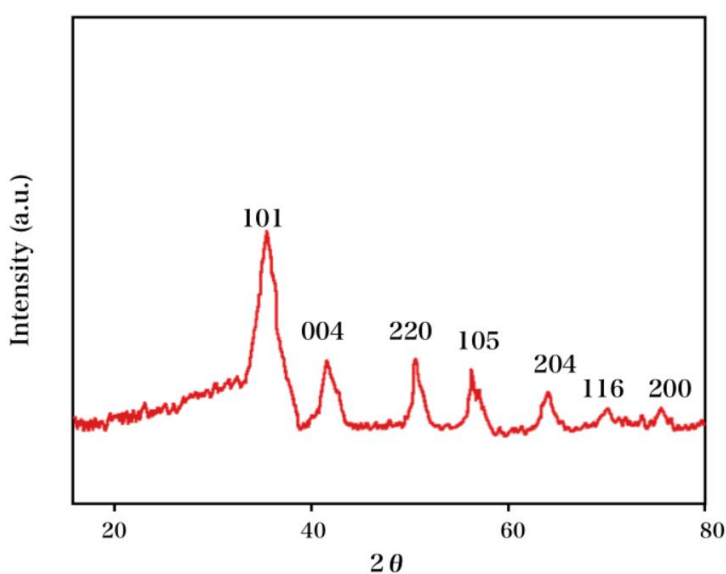
The crystal structure of the prepared samples was characterised using an X-ray diffractometer (D8 –Advance XRD, Bruker, Germany) with Cu K $\alpha$  radiation. Electrochemical measurements were carried out based on GCE using a CH Instruments 660A electrochemical Workstation (CHI-660 A, CH Instruments, Texas, USA). After polishing using an alumina-water slurry, the GCE was rinsed with ethanol and water. The surface of the GCE was modified by dropping 7  $\mu$ L of the 1 mg/mL catalyst dispersion onto the GCE, followed by drying at ambient temperature. The workstation was equipped with a three-compartment geometry, where the reference and auxiliary electrodes were Ag/AgCl (3 M KCl) electrodes and a platinum wire. All electrochemical experiments were performed at ambient temperature.

#### 2.4. Blood sample preparation

Blood specimens were collected in heparinised tubes, followed by immediate centrifuging at 3000 g for 10 min. Prior to testing, the plasma was stored at  $-20\text{ }^{\circ}\text{C}$ . A 1 mL plasma sample was mixed with NaOH (1 mL, 2 M) and clozapine (10  $\mu\text{L}$ , 20  $\mu\text{g}/\text{mL}$ ; internal standard (I.S.)). After a 10 s vortex-mix, the tubes were added to 4 mL of 99:1 diisopropyl ether–isoamylalcohol (v/v; extraction solvent). The mixed solution was shaken for 10 min and centrifuged for 10 min at  $4\text{ }^{\circ}\text{C}$  and 3000 g. The tubes containing 150  $\mu\text{L}$  of 0.1 M  $\text{KH}_2\text{PO}_4$  (pH 2.2; with 25%  $\text{H}_3\text{PO}_4$ ) were mixed with the organic phase at 250 cycles/min for 5 min, followed by centrifuging for 2 min at 3000 g. The upper organic layer was carefully aspirated for analysis.

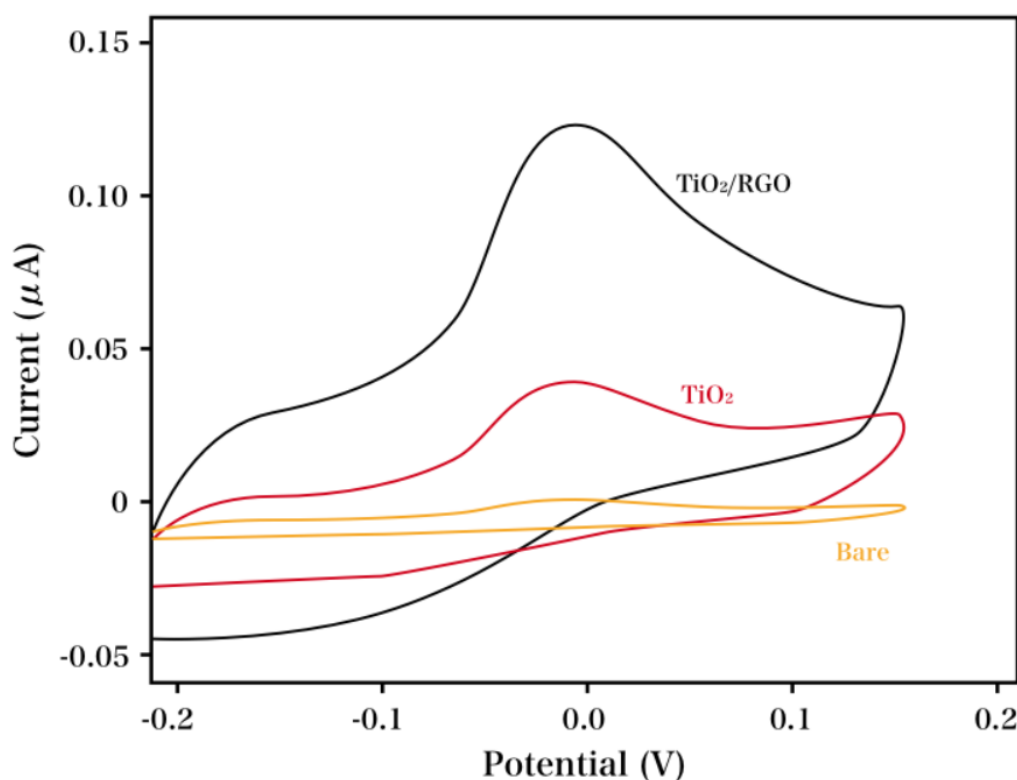
### 3. RESULTS AND DISCUSSION

The RGO-TiO<sub>2</sub> was characterised via XRD and is shown in Fig. 1. The characteristic peaks observed at  $2\theta$  of  $25.1^{\circ}$ ,  $37.3^{\circ}$ ,  $47.7^{\circ}$ ,  $54.2^{\circ}$ ,  $54.7^{\circ}$ ,  $62.4^{\circ}$ ,  $68.1^{\circ}$ ,  $70.7^{\circ}$  and  $75.1^{\circ}$  resulted from the (101), (004), (200), (105), (211), (204), (116), (200), and (215) crystallographic planes of anatase, respectively, according to Fu and co-workers (2014). It was observed that all samples were primarily composed of the anatase TiO<sub>2</sub> phase and showed no diffraction peaks of a GO layered structure; this might be due to the disappearance of layer-stacking regularity after reduction or the low amount and relatively low diffraction intensity of graphene [43]. In addition, a broad peak overlapping the (101) plane of anatase was observed and suggested the incorporation of TiO<sub>2</sub> with the exfoliated RGO sheets.



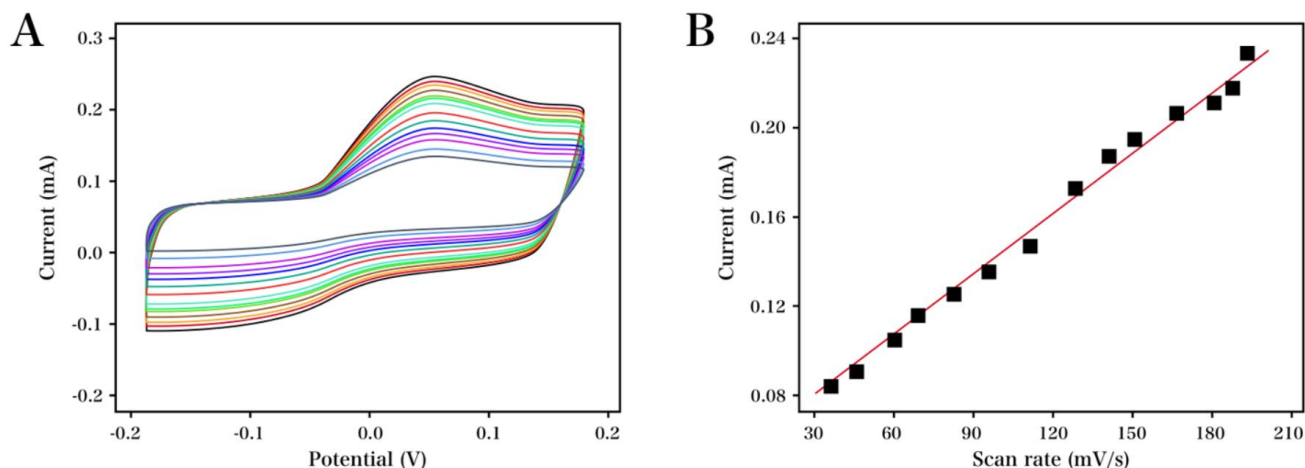
**Figure 1.** XRDs recorded for RGO-TiO<sub>2</sub> nanohybrid.

A comparative study was carried out on the electrocatalytic detection performance of the bare,  $\text{TiO}_2$ , and RGO- $\text{TiO}_2$  modified GCE in 0.1 M of pH 8 PBS containing 50 ng/mL 9-hydroxyrisperidone. The cyclic voltammograms (CVs) in Fig. 2 displayed no significant current response for 9-hydroxyrisperidone over an applied potential range of  $-0.2$  to  $0.2$  V, whereas the  $\text{TiO}_2$  modified GCE showed a direct oxidation peak of 9-hydroxyrisperidone at an applied potential of  $0.08$  V. This indicated an enhanced electrochemical reaction rate on the surface of the electrode in the presence of the as-prepared  $\text{TiO}_2$ . Additionally, a comparable CV shape was found at the GCE after modification with RGO- $\text{TiO}_2$ , with an enhanced current and decreased oxidation peak potential ( $0.02$  V). This suggested that the catalytic oxidation of 9-hydroxyrisperidone could be enhanced after the  $\text{TiO}_2$  was incorporated into the RGO.



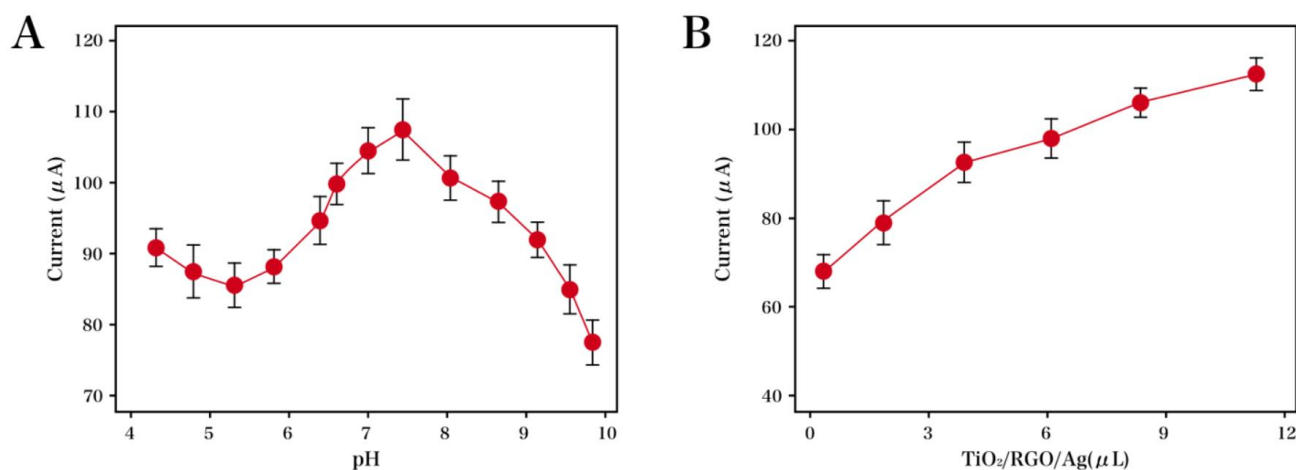
**Figure 2.** CVs recorded for the bare GCE,  $\text{TiO}_2$  modified GCE, and RGO- $\text{TiO}_2$  modified GCE in 0.1 M PBS containing 50 ng/mL of 9-hydroxyrisperidone (scan rate of 50 mV/s).

Fig. 3 shows different peak currents of 9-hydroxyrisperidone using the RGO- $\text{TiO}_2$  modified GCE with varying scan rates. The oxidation current increased as the scan rate increased. The scan rate is linearly related to the oxidation current, obeys the following equation:  $I_{pa} (\mu\text{A}) = 0.84705v + 75.77$  ( $R^2 = 0.997$ ), suggesting that the electrode surface reaction is adsorption-controlled. Additionally, as the scan rate increased, a gradual shift to the positive direction was found for the anodic peak potential. The linearity of the logarithm of scan rate and the oxidation potential is described by the following equation:  $E_{pa} (\text{V}) = 0.02687 \log v (\text{V/s}) + 0.02014$  ( $R^2 = 0.9904$ ). Two electrons are involved in this reaction (according to the Laviron's equation), which is consistent with a previous study [44].



**Figure 3.** (A) CVs recorded for the RGO-TiO<sub>2</sub> modified GCE in 0.1 M PBS containing 50 ng/mL of 9-hydroxyrisperidone. Scan rate: 20—200 mV/s; (B) Plots of peak currents vs. the scan rate.

The influence of the electrolyte pH on the oxidation of the 9-hydroxyrisperidone at the modified electrode has been reported previously. Only a non-significant dependence on pH value was observed through CV measurement, which was consistent with the result of a previous report using carbon electrodes at an applied potential [45]. The influence of pH (4–10) on the analysis of the 9-hydroxyrisperidone (50 ng/mL) using the RGO-TiO<sub>2</sub> modified GCE is shown in Fig. 4A. As the pH increased from 5.5 to 8, a gradual increase in the current response was observed but decreased after that. Therefore, the oxidation of 9-hydroxyrisperidone was optimised at a pH of 8. These results confirmed the involvement of 2 electrons in the first step. Two oxidation steps constitute the complete oxidation processes, where the second one refers to a  $2e^-$ ,  $2H^+$  oxidation, and involves  $4e^-$  and  $4H^+$  overall [46–48]. In addition, we also studied the influence of modifier amount on the anodic peak current of the 9-hydroxyrisperidone.



**Figure 4.** Plot of  $I_{pa}$  against (A) PBS pH value (B) amount of modifier for the analysis of 9-hydroxyrisperidone.

As the modifier amount increased, the anodic peak current sharply increased (Fig. 4B). The maximum peak current was found at 7  $\mu\text{L}$ ; the current response decreased with an additional modifier that is ascribed to the additional time it takes for the 9-hydroxyrisperidone electrons to travel through the thicker RGO-TiO<sub>2</sub> film.

The characteristic amperometric response of the RGO-TiO<sub>2</sub> modified GCE after successively adding the 9-hydroxyrisperidone is shown in Fig. 5. After each addition of 9-hydroxyrisperidone, a rapid increase in the current response was observed, followed by a steady-state within 3 s. This suggested a rapid response of the RGO-TiO<sub>2</sub>/GCE towards the 9-hydroxyrisperidone. The relationship between 9-hydroxyrisperidone (1 to 150 ng/mL) and the current response is linear and shown in the calibration graph of the inset, with a regression equation of  $I (\mu\text{A}) = 0.09414 C(\text{ng/mL}) + 10.74$  ( $R_2 = 0.993$ ). Based on a signal to noise ratio of 3, the limit of detection (LOD) was determined to be 0.52 ng/mL. To allow for comparison to previous reports, the characteristics of different electrochemical sensors for 9-hydroxyrisperidone are summarised in Table 1.

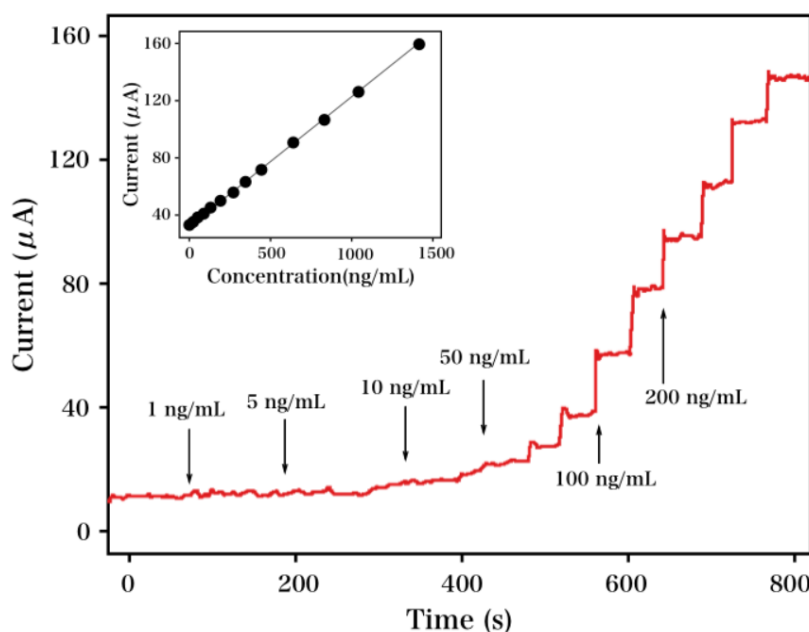


**Figure 5.** Amperometric response recorded for the RGO-TiO<sub>2</sub> modified GCE after successively adding the 9-hydroxyrisperidone at a potential of  $-0.02$  V. Inset shows the calibration curve (concentration range: 1–1500 ng/mL).

**Table 1.** Comparison of the major characteristics of sensors used for the detection of 9-hydroxyrisperidone.

Electrode	Linear detection range	Detection limit	Reference
HPLC + coulometric detection	2 - 100 ng/mL	1 ng/mL	[22]
LC-MS-MS	0.1 - 250 ng/mL	—	[49]
HPLC + UV absorbance detection	5 - 100 ng/mL	2 ng/mL	[50]
RGO-TiO <sub>2</sub> modified GCE	1 - 150 ng/mL	0.52 ng/mL	This work

The feasibility and practicability of our developed biosensor were investigated using ten clinical human blood plasma specimens. At least three times of measurements were carried out on each specimen. Table 2 clearly shows the high reliability and feasibility of this biosensor (relative errors < 5%), and suggests a great potential for this technique to be used in clinical analysis.

**Tab. 2.** Detection performance of our developed technique toward clinical human blood plasma specimens.

Sample	Added (ng/mL)	Detected (ng/mL)	Recovery (%)	RSD (%)
1	20	20.41	102.05	4.7
2	40	39.78	99.45	3.1
3	80	81.02	101.27	1.9

#### 4. CONCLUSIONS

In the present report, an RGO-TiO<sub>2</sub> electrode was prepared using a simple wet chemical strategy and applied to the fabrication of a biosensor towards 9-hydroxyrisperidone. The electro catalytic activity of our developed biosensor to the 9-hydroxyrisperidone oxidation was higher than that of bare and TiO<sub>2</sub> modified GCEs. The lower oxidation potential and enhanced oxidation current resulted from the synergy between TiO<sub>2</sub> and RGO. In conclusion, our developed biosensor exhibited a low LOD, wide linear detection range, and fast current response.

#### References

1. S.V. Bowskill, S.A. Handley, D.S. Fisher, R.J. Flanagan and M.X. Patel, *Therapeutic Drug Monitoring*, 34 (2012) 349.
2. R. Mandrioli, L. Mercolini, D. Lateana, G. Boncompagni and M.A. Raggi, *Journal of Chromatography B Analytical Technologies in the Biomedical & Life Sciences*, 879 (2011) 167.
3. C.M. Sherwin, S.N. Saldaña, R.R. Bies, M.G. Aman and A.A. Vinks, *Therapeutic Drug Monitoring*, 34 (2012) 535.
4. A.J. Schmidt, J.C. Krieg, H.W. Clement, U.M. Hemmeter, E. Schulz, H. Vedder and P. Heiser, *Journal of Psychopharmacology*, 24 (2010) 349.
5. C.A. Calarge and D.D. Miller, *Journal of Child & Adolescent Psychopharmacology*, 21 (2011) 163.
6. X. Zhang, X. Zhao, C. Zhang, L. Yang, X. Xiong, Y. Zhou, Y. Yang and J. Duan, *Chroma*, 71 (2010) 1015.
7. H.D. Yoo, H.Y. Cho, S.N. Lee, H. Yoon and Y.B. Lee, *J Pharmacokinet Pharmacodyn*, 39 (2012) 329.
8. N. Vanwong, N. Ngamsamut, S. Medhasi, A. Puangpetch, M. Chamnanphon, T. Tan-Kam, Y. Hongkaew, P. Limsila and C. Sukasem, *J Child Adolesc Psychopharmacol*, 27 (2016) 185.
9. L.I. Hong-Xia, D.J. Yang, D. Fan, X.Q. Wang and X.W. Xing, *West China Journal of Pharmaceutical Sciences*, 26 (2011) 369.
10. F. Lancelin, E. Bourcier, M.V. Le, Y. Lemeille, S. Brovedani, P. Paubel and M.L. Piketty, *Therapeutic Drug Monitoring*, 32 (2010) 757.
11. J. Jia, M. Zhang, L.U. Xiaopei, L.U. Chuan, L.I. Shuijun, G. Liu and Y.U. Chen, *Chinese Journal of Clinical Pharmacy*, (2010)



12. S.K.M. Siva and M. Ramanathan, *Biomedical Chromatography BMC*, 30 (2016) 263.
13. N. Ngamsamut, Y. Hongkaew, N. Vanwong, P. Srisawasdi, A. Puangpetch, B. Chamkrachangpada, T. Tan-Khum, P. Limsila and C. Sukasem, *Basic & Clinical Pharmacology & Toxicology*, 33 (2016) 267.
14. W. Xu, G. E. Wright, M. Yanachkova and I. B. Yanachkov, *Letters in Organic Chemistry*, 11 (2014) 470.
15. D.S. Yang, S.J. Seong, Y.R. Yoon, M.S. Lim, K.H. Kwak and S.J. Lee, *Journal of Psychopharmacology*, 28 (2014) 341.
16. A.M. Wessels, B.G. Pollock, N.G. Anyama, L.S. Schneider, J.A. Lieberman, S.R. Marder and R.R. Bies, *J Clin Psychopharmacol*, 30 (2010) 683.
17. S. Millefiori and A. Alparone, *European Journal of Medicinal Chemistry*, 45 (2010) 1367.
18. L.G. Sidelnikova, V.A. Kartashov, L.V. Chernova, L.G. Sidelnikova, V.A. Kartashov, L.V. Chernova, L.G. Sidelnikova, V.A. Kartashov, L.V. Chernova and L.G. Sidelnikova, (2015) 34.
19. T.K. Keeton, H. Krutzsch and W. Lovenberg, *Catecholamines Basic & Clinical Frontiers*, (1979) 871.
20. M.J. Le, S. Edouard and J.C. Levron, *Journal of Chromatography B Biomedical Sciences & Applications*, 614 (1993) 333.
21. T. Nagasaki, T. Ohkubo, K. Sugawara, N. Yasui, H. Furukori and S. Kaneko, *Journal of Pharmaceutical & Biomedical Analysis*, 19 (1999) 595.
22. D.S. Schatz and A. Saria, *Pharmacology*, 60 (2000) 51.
23. B.M. Remmerie, L.L. Sips, V.R. De, J.J. De, A.M. Schothuis, E.W. Hooijschuur and V.D.M. Nc, *Journal of Chromatography B Analytical Technologies in the Biomedical & Life Sciences*, 783 (2003) 461.
24. M. Aravagiri and S.R. Marder, *Journal of Mass Spectrometry Jms*, 35 (2000) 718.
25. M.M. De, B.M. Remmerie, V.R. De, L.L. Sips, S. Boom, E.W. Hooijschuur, V.D.M. Nc and P.M. Timmerman, *Journal of Chromatography B Analytical Technologies in the Biomedical & Life Sciences*, 870 (2008) 8.
26. B. Čabovska, S.L. Cox and A.A. Vinks, *Journal of Chromatography B Analytical Technologies in the Biomedical & Life Sciences*, 852 (2007) 497.
27. K. Titier, E. Déridet, E. Cardone, A. Abouelfath and N. Moore, *Journal of Chromatography B Analytical Technologies in the Biomedical & Life Sciences*, 772 (2002) 373.
28. Aslam M S, Rehman R, Bashir A Choudhary, et al. *ANTIFUNGAL, CYTOTOXIC AND PHYTOTOXICITY OF AERIAL PART OF RANUNCULUS MURICATUS*[J]. *Universal Journal of Pharmaceutical Research*, 2016, 1(1):7-12.
29. Kaijian Hou, Chuanjian Lin, Chao Chen, Bangtai Wu, et al. *Association of probiotics and bone mineral density in Chinese patients with type 2 diabetes. biomedical research India*.2017.1.
30. Chioma E D, Chioma E D, Chioma E D. *FORMULATION AND EVALUATION OF ETODOLAC NIOSOMES BY MODIFIED ETHER INJECTION TECHNIQUE*[J]. *Universal Journal of Pharmaceutical Research*, 2016, 1(1):1-6.
31. N. Liu, H. Wu, M.T. McDowell, Y. Yao, C. Wang and Y. Cui, *Nano Letters*, 12 (2012) 3315.
32. J.A. Lichter, K.J.V. Vliet and M.F. Rubner, *Macromolecules*, 42 (2016) 8573.
33. I. Dincer and C. Acar, *International Journal of Hydrogen Energy*, 40 (2015) 11094.
34. M.J. Shearer and P. Newman, *Journal of Lipid Research*, 55 (2014) 345.
35. G.D.O. Neto, L.R. Júnior and L.T. Kubota, *Electroanalysis*, 11 (2015) 527.
36. D. Ivnitiski, I. Abdel - Hamid, P. Atanasov, E. Wilkins and S. Stricker, *Electroanalysis*, 12 (2015) 317.
37. Y. Song, Y. Luo, C. Zhu, H. Li, D. Du and Y. Lin, *Biosensors & bioelectronics*, 76 (2015) 195.
38. P. Zhang, X. Zhao, Y. Ji, Z. Ouyang, X. Wen, J. Li, Z. Su and G. Wei, *Journal of Materials Chemistry B*, 3 (2015) 2487.
39. J. Pezard, M. Lazar, N. Haddour, C. Botella, P. Roy, J.B. Brubach, D. Wysocka, B. Vilquin, P.R.

- Romeo and F. Buret, *Thin Solid Films*, 617 (2016) 150.
40. M.M. Barsan and C.M.A. Brett, *Studia Universitatis Babes-Bolyai Chemia*, 60 (2015) 31.
41. A.A. Ensafi, M. Sohrabi, M. Jafari-Asl and B. Rezaei, *Appl. Surf. Sci.*, 356 (2015) 301.
42. R. Shrivastava, S. Saxena, S.P. Satsangee and R. Jain, *Ionics*, 21 (2015) 2039.
43. J. Du, X. Lai, N. Yang, J. Zhai, D. Kisailus, F. Su, D. Wang and L. Jiang, *ACS nano*, 5 (2010) 590.
44. S. Yang, G. Li, Y. Yin, R. Yang, J. Li and L. Qu, *Journal of Electroanalytical Chemistry*, 703 (2013) 45.
45. G.A. Mersal, *Food Analytical Methods*, 5 (2012) 520.
46. R.S. Nunes and É.T. Cavaleiro, *Journal of the Brazilian Chemical Society*, 23 (2012) 670.
47. N. Spataru, B.V. Sarada, D.A. Tryk and A. Fujishima, *Electroanalysis*, 14 (2002) 721.
48. J.-Y. Sun, K.-J. Huang, S.-Y. Wei, Z.-W. Wu and F.-P. Ren, *Colloids and Surfaces B: Biointerfaces*, 84 (2011) 421.
49. B.M. Remmerie, L.L. Sips, V.R. De, J.J. De, A.M. Schothuis, E.W. Hooijschuur and V.D.M. Nc, *Journal of Chromatography B*, 783 (2003) 461.
50. A. Avenoso, G. Facciola, M. Salemi and E. Spina, *Journal of Chromatography B Biomedical Sciences & Applications*, 746 (2000) 173

© 2018 The Authors. Published by ESG ([www.electrochemsci.org](http://www.electrochemsci.org)). This article is an open access article distributed under the terms and conditions of the Creative Commons Attribution license (<http://creativecommons.org/licenses/by/4.0/>).